J. Phys. Chem. A **2006,** *110,* 11627−11635

Generation of Gas-Phase VO^{2+}, $VOOH^{+}$, and VO_2^{+}−Nitrile Complex Ions by Electrospray Ionization and Collision-Induced Dissociation

Zack Parsons,[†] Chris Leavitt,[†] Thanh Duong,[†] Gary S. Groenewold,[‡] Garold L. Gresham,[‡] and Michael J. Van Stipdonk*,[†]

Department of Chemistry, Wichita State University, Wichita, Kansas 67260-0051, and Idaho National Laboratory, Idaho Falls, Idaho 83415-2208

Received: May 5, 2006; In Final Form: July 26, 2006

Cationic metal species normally function as Lewis acids, accepting electron density from bound electron-donating ligands, but they can be induced to function as electron donors relative to dioxygen by careful control of the oxidation state and ligand field. In this study, cationic vanadium(IV) oxohydroxy complexes were induced to function as Lewis bases, as demonstrated by addition of O_2 to an undercoordinated metal center. Gas-phase complex ions containing the vanadyl (VO^{2+}), vanadyl hydroxide ($VOOH^{+}$), or vanadium(V) dioxo (VO_2^{+}) cation and nitrile (acetonitrile, propionitrile, butyronitrile, or benzonitrile) ligands were generated by electrospray ionization (ESI) for study by multiple-stage tandem mass spectrometry. The principal species generated by ESI were complexes with the formula $[VO(L)_n]^{2+}$, where L represents the respective nitrile ligands and $n = 4$ and 5. Collision-induced dissociation (CID) of $[VO(L)_5]^{2+}$ eliminated a single nitrile ligand to produce $[VO(L)_4]^{2+}$. Two distinct fragmentation pathways were observed for the subsequent dissociation of $[VO(L)_4]^{2+}$. The first involved the elimination of a second nitrile ligand to generate $[VO(L)_3]^{2+}$, which then added neutral H_2O via an association reaction that occurred for all undercoordinated vanadium complexes. The second $[UO(L)_4]^{2+}$ fragmentation pathway led instead to the formation of $[VOOH(L)_2]^{+}$ through collisions with gas-phase H_2O and concomitant losses of L and $[L + H]^{+}$. CID of $[VOOH(L)_2]^{+}$ caused the elimination of a single nitrile ligand to generate $[VOOH(L)]^{+}$, which rapidly added O_2 (in addition to H_2O) by a gas-phase association reaction. CID of $[VONO_3(L)_2]^{+}$, generated from spray solutions created by mixing $VOSO_4$ and $Ba(NO_3)_2$ (and precipitation of $BaSO_4$), caused elimination of NO_2 to produce $[VO_2(L)_2]^{+}$. CID of $[VO_2(L)_2]^{+}$ produced elimination of a single nitrile ligand to form $[VO_2(L)]^{+}$, a V(V) analogue to the O_2-reactive V(IV) species $[VOOH(L)]^{+}$; however, this V(V) complex was unreactive with O_2, which indicates the requirement for an unpaired electron in the metal valence shell for O_2 addition. In general, the $[VO_2(L)_2]^{+}$ species required higher collisions energies to liberate the nitrile ligand, suggesting that they are more strongly bound than the $[VOOH(L)_2]^{+}$ counterparts.

Introduction

The addition of dioxygen to metal centers has attracted the interest of chemists for decades,[1−4] on account of its importance to oxidation in biological systems, including oxygen transport by hemoglobin.[5] Generally, cationic metals would be expected to act as Lewis acids, forming ligand complexes with nucleophilic ligands. However, in a surprising number of cases, cationic metal species having higher-lying oxidation states will also function as electron donors with respect to dioxygen. This has been demonstrated for transition-metal cluster cations in the gas phase.[6,7] Binding of dioxygen to transition metals is dependent on the oxidation state and on the ligands attached to the metal center, as has been demonstrated for Fe in biological systems.[4,8,9] Yet, in general, definitively establishing the effect of oxidation state and ligation on metal reactivity patterns is a complicated task. However, recent research demonstrated ligand- and oxidation-state-sensitive formation of dioxygen complexes with reduced, gas-phase $[UO_2]^{+}$ species.[10] This suggests that gas-phase vanadium(IV) oxo species might be reactive with dioxygen, because, like $[UO_2]^{+}$, $[VO]^{+}$ has a single unpaired valence electron whose reactivity might be adjustable by changes in the metal ligand field.

In general terms, the intrinsic chemistry of vanadium and vanadium-containing complexes is a topic of interest in both biology and industrial chemistry. Vanadium is a trace element present in animal and plant cells,[11] where it serves as the reactive center in a variety of enzymes including some haloperoxidases[11−16] and nitrogenases in some nitrogen-fixing bacteria;[17] these discoveries have motivated a wide range of studies using model compounds.[18−21] In industry, vanadium oxides are employed in processes ranging from the oxidative dehydrogenation of alkanes to the oxidation of alkylaromatics, alcohols, and SO_2,[22,23] the latter being the crucial step in the modern production of sulfuric acid.[24]

The reactivity of oxovanadium species in catalytic and biochemical reactions has motivated several studies of model systems in the gas phase using mass spectrometry.[25−39] Early on, Muller and Benninghoven showed that a variety of oxyvanadium ions could be formed using secondary ion mass spectrometry, providing a desorption approach for ion formation.[40] Since then, detailed bond enthalpy data have been

* To whom correspondence should be addressed. Address: Department of Chemistry, Wichita State University, Wichita, KS 67260-0051. Phone: 316-978-7381. Fax: 316-978-3431. E-mail: Mike.VanStipdonk@wichita.edu.

† Wichita State University.

‡ Idaho National Laboratory.

10.1021/jp062769p CCC: $33.50
Published on Web 09/26/2006

generated for noncovalent complexes consisting of bare vanadium cations ligated with water, amines, and oxygen.[41] Castleman and co-workers examined the formation and bond dissociation thresholds of vanadium oxide cluster ions[28] and the reactions of the $V_nO_m^+$ cations with small fluorinated hydrocarbons[25,26] or ethane and ethylene.[29] Schwarz and co-workers examined systems as diverse as small vanadium cluster cations and molecular oxygen;[32] the formation and energetics of VO^{2+}, VOH^{2+}, and $[V,O,H_2]^{2+}$;[35] the ion chemistry of gas-phase vanadyl methoxy and alkoxy(catecholato) complexes;[31,32] and the oxidation of alkanes by VO_2^+ and small vanadium oxide cations.[30,33] Cluster ions containing multiple vanadium atoms have also received attention: careful experiments by Armentrout and co-workers produced metal−metal, metal−H, and metal−O bond enthalpies for ionic V_n clusters.[42] Fielicke and Rademann examined the stability and reactivity patterns of vanadium oxide cluster ions with between 4 and 14 vanadium atoms, including reactions with a range of hydrocarbons and small molecules such as NO and SO_2.[36] Dinca and co-workers showed the size-selective reactivity of $V_xO_y^-$ clusters with alkyl esters and found that undercoordinated vanadium metal centers would add H_2O even though the cluster charge was negative.[43] More recent studies have focused on characterizing the structure of oxovanadium cluster cations using infrared multiphoton dissociation.[37−39]

In the present study, we explored the use of electrospray ionization (ESI) to generate gas-phase vanadyl (VO^{2+}), vanadyl hydroxide ($VOOH^+$), and vanadium(V) dioxo (VO_2^+) cations complexed with nitrile ligands [acetonitrile (acn), propionitrile (pn), butyronitrile (bn), and benzonitrile (bzn)]. Prior studies have demonstrated the utility of ESI for the production of oxovanadium ions for study in the gas phase. For example, Schröder and co-workers used ESI to generate a gas-phase methoxo-oxovanadium cluster for subsequent study of its gas-phase chemistry.[44] Bortolino and co-workers used ESI and mass spectrometry to study vanadium bromoperoxidase mimics in the gas phase[18,19] and produced evidence for gas-phase solvent-coordinated peroxovanadium clusters ions.[45] As we report here, ESI of aqueous solutions of vanadyl sulfate ($VOSO_4$) with the organonitriles as cosolvents generates doubly charged gas-phase complexes with the general formula $[VO(L)_n]^{2+}$, where L represents the respective nitrile ligands and $n = 4$ and 5. Also observed in the ESI spectra are ions with the general formula $[VOOH(L)_2]^+$. We found that species with the formula $[VO_2(L)_2]^+$ can be generated by collision-induced dissociation (CID) of $[VONO_3(L)_2]^+$ via the elimination of NO_2 and oxidation of the vanadyl ion to the vanadium(V) dioxocation. The nitrile-coordinated VO^{2+}, $VOOH^+$, and VO_2^+ cations were subjected to multiple-stage CID to probe fragmentation behavior. The combination of ESI and CID performed in a quadrupole ion trap enables the formation of a series of ions that vary in terms of extent of ligation, oxidation state, oxo form, and metal oxidation state. A limitation of the ion trap is that the kinetic energy distributions of the ions are not well-known, which hinders the measurement of ligand binding energies. However, the tremendous versatility of the ion trap for ion formation provides access to ion series that enables reactivity with H_2O and O_2 to be probed as the ion chemistry is systematically varied.

Experimental Methods

ESI-MS and multiple-stage CID were carried out using procedures established previously for the generation of gas-phase uranyl ion−ligand complexes.[46−50] Vanadyl sulfate hydrate [$VOSO_4 \cdot xH_2O$ (25% vanadium] and barium nitrate dihydrate [$Ba(NO_3)_2 \cdot 2H_2O$] were purchased from Acros Chemical and used as received. Acetonitrile, propionitrile, butyronitrile, and benzonitrile were purchased from Aldrich Chemical (St. Louis, MO) and used as received. Stock solutions of $VOSO_4$ and $Ba(NO_3)_2$ (ca. 1 mM concentration) were prepared by dissolving the appropriate amount of solid in deionized H_2O. Spray solutions for the generation of VO^{2+}−nitrile complexes by ESI were prepared by combining portions of the $VOSO_4$ stock solution and nitrile in a 1:100 relative molar ratio. For 1 mL of total solution volume, the amount of nitrile added ranged from ~5 to 8 μL because of the different densities of the nitriles used. These volumes of nitrile were sufficient to generate abundant doubly charged VO^{2+} complex ions, but low enough to avoid the introduction of significant partial pressures of neutral nitrile into the ion-trap instrument to participate in ion−molecule association reactions.

To prepare solutions used to generate gas-phase $VONO_3$−nitrile complexes, equal volumes of equimolar solutions of $VOSO_4$ and $Ba(NO_3)_2$ were combined in a beaker. A white precipitate ($BaSO_4$) immediately formed and was allowed to settle over a period of several hours. The $BaSO_4$ precipitate was filtered, and 1-mL portions of the resulting supernatant were combined with appropriate volumes of the nitriles for the ESI experiments.

ESI mass spectra were collected using a Finnigan LCQ-Deca ion-trap mass spectrometer (ThermoFinnigan Corporation, San Jose, CA). The spray solutions were delivered to the ESI source through fused-silica capillaries and a syringe pump at a flow rate of 3−5 μL/min. The atmospheric-pressure ionization stack settings for the LCQ instrument (lens voltages, quadrupole and octapole voltage offsets, etc.) were optimized for maximum ion transmission to the ion-trap mass analyzer by using the autotune routine within the LCQ Tune program. The spray needle voltage was maintained at +5 kV, and the N_2 sheath gas flow at 25 units (approximately 0.375 L/min). For most experiments, the heated capillary, used for ion desolvation prior to injection into the ion trap, was maintained at 120 °C to maximize both the total ion signal and the production of doubly charged complexes. Helium was used as the bath/buffer gas to improve trapping efficiency and as the collision gas for CID experiments. Ion charge states were confirmed by examining the isotopic peak spacing using the ZoomScan high-resolution function of the LCQ-Deca instrument. Doubly charged species were identified by isotopic (primarily ^{12}C and ^{13}C from the nitrile ligands) peak spacing of 0.5 mass units (u).

The CID (MS/MS and MS^n) experiments were performed as follows: Precursor ions were selected and isolated for activation using isolation widths of 0.7−1.2 mass units centered on the m/z value of the precursor ion. The isolation width for a given complex ion was chosen empirically to provide an optimal compromise between abundant ion signal and the isolation of single isotopic precursor ion peaks. The normalized collision energy (a term arbitrary to the LCQ system that represents a percentage of 5 V, normalized for precursor ion mass, applied to the end-cap electrodes to increase ion kinetic energy) was set between 20% and 30% of a mass-normalized collision energy. Given the respective masses of the VO^{2+}, $VOOH^+$, and VO_2^+ nitrile complexes, the applied collision voltages ranged from 0.43 to 0.87 V (laboratory frame) depending on the number and type of nitrile ligands. In most cases, except where specifically indicated, applied collision voltages of this magnitude were sufficient to reduce the precursor ion intensity to ~10% relative abundance. Where relevant to the discussion of ion dissociation, the energies used to affect CID are provided in volts, laboratory frame, without the correction for precursor

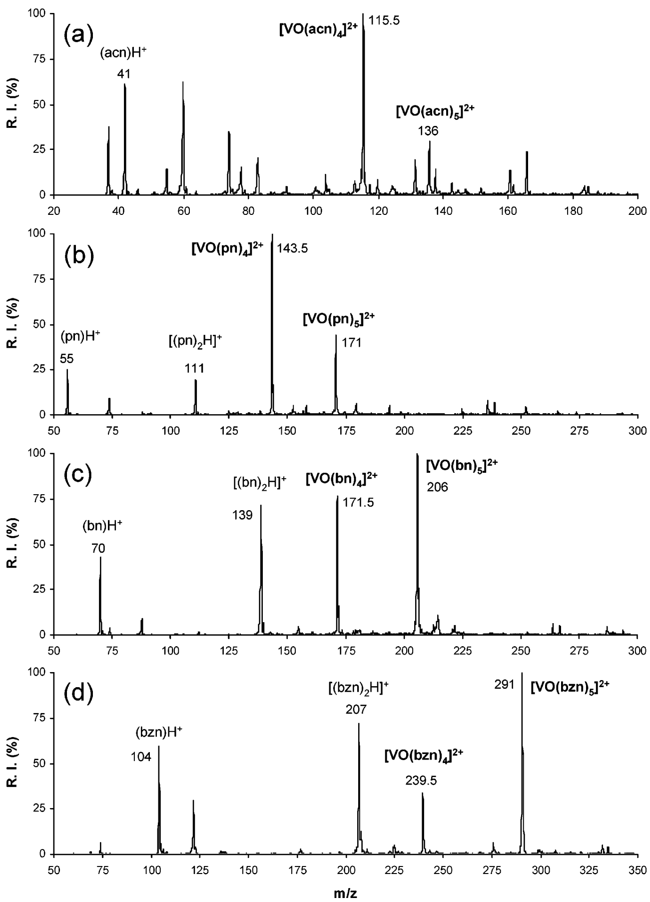

Figure 1. ESI spectra produced from aqueous solutions containing $VOSO_4$ and (a) acetonitrile, (b) propionitrile, (c) butyronitrile, and (d) benzonitrile. In the spectra, only the nitrile and VO^{2+}−nitrile complex ions are labeled. In spectrum a, the majority of the unlabeled peaks correspond to protonated solvent complexes.

ion mass. The activation *Q* (used to adjust the q_z value for the resonant excitation of the precursor ion during the CID experiment) was set in these experiments at 0.3 to ensure effective trapping and collisional activation. The activation time for all CID experiments was 30 ms. Following the isolation/activation period, the precursor and product ions were scanned out of the trap and detected as part of the automated mass-analysis operation.

The pressure within the vacuum system was ca. 1.2×10^{-5} Torr during experimental trials, with He as the principal collision/bath gas. H_2O was present as an indigenous species in the vacuum system and was admitted into the vacuum system directly because of its use as in the spray solvent mixture. The partial pressure of H_2O was estimated to be ca. 1×10^{-6} Torr based on previous hydration studies using similar operating parameters.[49] To confirm the formation of O_2 adducts formed via ion−molecule association reactions, a He/O_2 blend (certified 0.1% O_2, Linweld, Wichita, KS) was used as the collision/buffer gas. To probe for gas-phase ligand-addition reactions, the complex ions were isolated using isolation widths similar to those outlined above. The normalized collision energy was set at 0%, and the activation time was varied from 1 to 1000 ms.

Results and Discussion

ESI Mass Spectra. Figure 1 shows the ESI spectra generated from aqueous solutions that were 1 mM $VOSO_4$ with 100-fold molar excesses of (a) acn, (b) pn, (c) bn, and (d) bzn. A summary of the relevant vanadium-containing ionic complexes (*m*/*z* ratios and proposed compositions) observed in the four spectra is provided in Table 1. The proposed complex ion compositions were confirmed using multiple-stage CID. As in earlier investigations of gas-phase uranyl species by our group,[49,50] we found that the general distribution of singly and doubly charged complex ions containing vanadium was influenced by the temperature of the heated capillary used in the LCQ-Deca instrument to desolvate the ions prior to their transmission to the ion-trap mass spectrometer. For example, at low desolvation temperatures of 100−125 °C, the dominant vanadium-containing ions observed were doubly charged vanadyl complexes with the general formula $[VO(L)_n]^{2+}$, where L corresponds to the respective nitriles and $n = 4$ and 5. Minor peaks (ca. 10% relative intensity or lower) corresponding to ions with the formula $[VOOH(L)_2]^{+}$ were also observed. At higher capillary/desolvation temperatures (ca. 200 °C), an increase of the relative intensities of the singly charged $[VOOH(L)_2]^{+}$ complex ions and a decrease of the $[VO(L)_n]^{2+}$ ion intensities were observed. We attribute this observation to the thermal dissociation, at high temperatures, of the doubly charged vanadyl (VO^{2+}) complexes to produce the singly charged vanadyl hydroxide (VOOH) species. As discussed below, the formation of $[VOOH(L)_n]^{+}$ is a dissociation pathway observed for the CID of $[VO(L)_4]^{2+}$. The best compromise between high overall ion signal and maximum production of doubly charged species was found at desolvation capillary temperatures between 100 and 120 °C. The spectra shown in Figure 1 were collected at 120 °C.

TABLE 1: ESI Spectral Data for the Relevant Vanadium-Containing Ionic Complexes

nitrile	ion *m*/*z* value	composition assignment
acetonitrile	95	$[VO(acn)_3]^{2+}$
	104	$[VO(acn)_3(H_2O)]^{2+}$
	115.5	$[VO(acn)_4]^{2+}$
	124.5	$[VO(acn)_4(H_2O)]^{2+}$
	136	$[VO(acn)_5]^{2+}$
	143	$[VOOH(acn)(H_2O)]^{+}$
	166	$[VOOH(acn)_2]^{+}$
propionitrile	116	$[VO(pn)_3]^{2+}$
	125	$[VO(pn)_3(H_2O)]^{2+}$
	143.5	$[VO(pn)_4]^{2+}$
	152.5	$[VO(pn)_4(H_2O)]^{2+}$
	171	$[VO(pn)_5]^{2+}$
	157	$[VOOH(pn)(H_2O)]^{+}$
	194	$[VOOH(pn)_2]^{+}$
butyronitrile	137	$[VO(bn)_3]^{2+}$
	146	$[VO(bn)_3(H_2O)]^{+}$
	171	$[VOOH)(bn)(H_2O)]^{+}$
	171.5	$[VO(bn)_4]^{2+}$
	206	$[VO(bn)_5]^{2+}$
	222	$[VOOH)(bn)_2]^{+}$
benzonitrile	188	$[VO(bzn)_3]^{2+}$
	205	$[VOOH(bzn)(H_2O)]^{+}$
	239.5	$[VO(bzn)_4]^{2+}$
	290	$[VOOH(bzn)_2]^{+}$
	291	$[VO(bzn)_4]^{2+}$

Because of the relatively low mass of acn (41 u), the VO^{2+}−acn complexes expected to be formed have *m*/*z* values such that they appear in the region of the ESI spectrum that is dominated, when low ion desolvation temperatures are used, by peaks attributable to protonated solvent monomers, dimers, and trimers. Nevertheless, as is apparent in Figure 1a, when acn was used in the ESI spray solvent, a prominent peak corresponding to $[VO(acn)_4]^{2+}$ was observed at *m*/*z* 115.5. A high-resolution scan of this peak confirmed the 2+ charge state. A peak corresponding to $[VO(acn)_5]^{2+}$ at *m*/*z* 136 appeared at a relative intensity of only 20−25%. Decreasing the capillary/desolvation temperature to values below 100 °C, or decreasing lens voltages for more “gentle” ion formation and transmission conditions, failed to appreciably increase the intensity of the $[VO(acn)_5]^{2+}$ species.

The $[VO(L)_4]^{2+}$ species was observed at *m/z* 143.5, 171.5, and 239.5 for pn (Figure 1b), bn (Figure 1c) and bzn (Figure 1d), respectively. Comparison of the spectra in Figure 1 demonstrates that the abundance of $[VO(L)_5]^{2+}$ increased, relative to that of $[VO(L)_4]^{2+}$, as the size of the nitrile ligand increased, and $[VO(L)_5]^{2+}$ was the dominant doubly charged complex ions observed for both bn and bzn. The number of ligands bound to the VO^{2+} cation is expected to be influenced by the relative strengths of ion−dipole/ion−induced dipole and charge-transfer attractive interactions, as well as ion−ligand and ligand−ligand repulsive interactions. The observed tendency to favor association with five nitriles over four in the gas-phase vanadyl complexes does not follow the trend in dipole moment or polarizability of the respective nitriles, but is consistent with differences in their proton affinity and gas-phase basicity (which are in the order acn < pn < bn < bzn).[51] This suggests that the overall number of ligands bound to the VO^{2+} ion is strongly dependent on the relative nucleophilic strengths of the various nitriles.

Despite the relatively low amount of nitrile used in the spray solvent system to generate the complex ions (ca. 1 vol %), only for the complexes containing acetonitrile were mixed species containing the nitrile and H_2O ligands observed. (For example, $[VO(acn)_3(H_2O)]^{2+}$ and $[VO(acn)_3(H_2O)_2]^{2+}$ were observed at *m/z* 104 and 124.5, respectively.) The low ion abundance of complexes containing H_2O ligands, particularly for complexes containing the larger nitriles, likely reflects the competition between nitrile and H_2O ligands (and the stronger basicity of the nitriles over H_2O) for coordination sites around the vanadyl ion in solution and during the ion-desolvation steps (on the LCQ platform, desolvation is effected both by an N_2 sheath gas and by the heated capillary) prior to the introduction of ions into the ion trap.

CID of $[VO(L)_n]^{2+}$, n = 4, 5. For each nitrile used in this study, CID (MS/MS stage) of $[VO(L)_5]^{2+}$ caused elimination of a single ligand to generate $[VO(L)_4]^{2+}$ (spectra not shown) as the sole fragmentation pathway. Product-ion spectra generated by the CID (MS^3 stage) of $[VO(L)_4]^{2+}$ are shown in Figure 2. In general, dissociation of $[VO(L)_4]^{2+}$ was observed to proceed via two reaction pathways: (a) reactions characterized by the elimination of a nitrile ligand and the formation of singly charged complex ions containing ligated $[VOOH]^+$ and (b) reactions characterized by the elimination of a single nitrile ligand, without charge reduction, to generate $[VO(L)_3]^{2+}$. For example, the most abundant product ion generated from the CID of $[VO(acn)_4]^{2+}$ (Figure 2a) was $[VOOH(acn)_2]^+$ at *m/z* 166. Formation of the vanadyl hydroxide species implicates collisions with H_2O, which is present as a contaminant in the He bath gas and also admitted directly into the ion-transmission optics and the vacuum system because of its use in the ESI spray solvent. The appearance of a peak at *m/z* 42 indicates that an acn ligand is eliminated as a protonated species during the dissociation reaction, which likely proceeds as suggested (in general terms) in reaction 1.

$$[VO(L)_4]^{2+} + H_2O \rightarrow [VO(L)_4(H_2O)]^{2+}* \leftrightarrow [VOOH(L)_2(L + H)(L)]^{2+}* \rightarrow [VOOH(L)_2]^+ + (L + H)^+ + L \quad (1)$$

CID of $[VO(acn)_4]^{2+}$ also caused the elimination of a single acn ligand to generate $[VO(acn)_3]^{2+}$ at *m/z* 95, which added

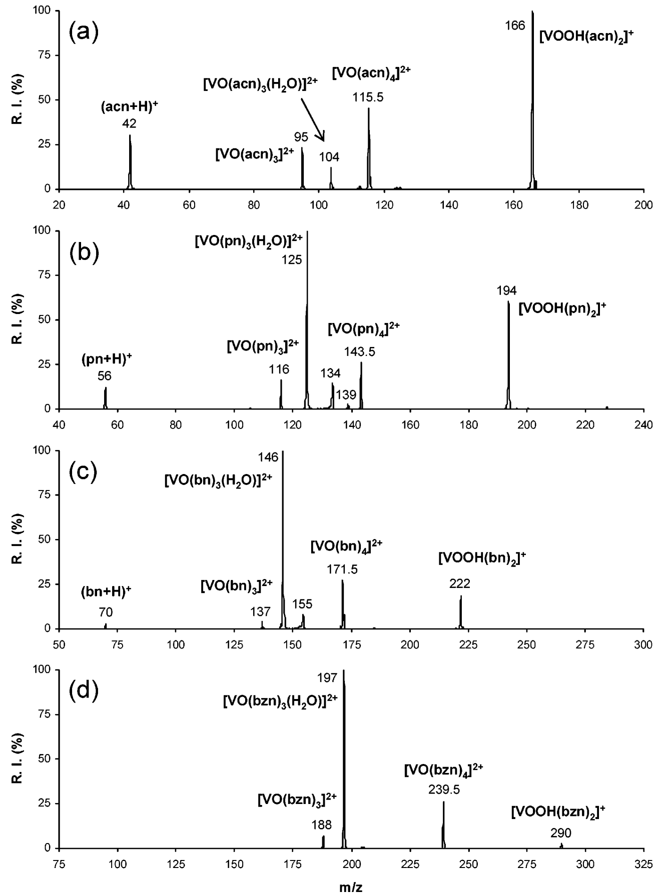

Figure 2. Collision-induced dissociation spectra of $[VO(L)_4]^{2+}$, where L corresponds to (a) acetonitrile, (b) propionitrile, (c) butyronitrile, and (d) benzonitrile. In b, the product ion at *m/z* 134 is the dihydrate species $[VO(pn)_3(H_2O)_2]^{2+}$, and the peak at *m/z* 139, $[VOOH(pn)]^+$, is a dissociation product of energetic $[VOOH(pn)_2]^{2+}$ at *m/z* 194. In c, the species at *m/z* 155 is the hydrate product $[VO(bn)_3(H_2O)]^{2+}$.

one and two H_2O ligands to produce $[VO(acn)_3(H_2O)]^{2+}$ and $[VO(acn)_3(H_2O)_2]^{2+}$ at *m/z* 104 and 113, respectively. The formation of the H_2O adducts by an ion−molecule reaction in the ion trap was confirmed by isolating and storing the $[VO(acn)_3]^{2+}$ species in the ion trap without imposed collisional activation (spectra not shown). The appearance of peaks 18 and 36 u higher in mass than the ion selected for storage is indicative of the generation of mono- and dihydrate species by gas-phase association reactions. The formation of hydrated ions is in accord with earlier investigations by our laboratory[46,47,49,50,52] and others[53−56] of the intrinsic reactions of ligated metal ions when isolated and stored in ion-trap mass spectrometers.

When pn, bn, and bzn were used in the spray solvent, the CID of $[VO(L)_4]^{2+}$ generated as the most abundant product ion the $[VO(L)_3(H_2O)]^{2+}$ species at *m/z* 125 (Figure 2b), 146 (Figure 2c), and 197 (Figure 2d), respectively. For pn and bn, the dihydrate species $[VO(L)_3(H_2O)_2]^+$ was also observed at *m/z* 134 and 155, respectively. The $[VO(L)_3]^{2+}$ ion was observed at relative intensities of only ca. 10−20%. Isolation and storage of $[VO(L)_3]^{2+}$ (MS^4 stage) in the ion trap for 30 ms, without imposed collisional activation, produced $[VO(L)_3(H_2O)]^{2+}$ at relative intensities comparable to those in Figure 2. This observation suggests that the hydrate was generated by the very rapid addition of H_2O to $[VO(L)_3]^{2+}$ once the latter species had been created from $[VO(L)_4]^{2+}$ by CID. Alternatively, the hydrated product ion might be generated by a collision-assisted substitution reaction in which a nitrile ligand is replaced by H_2O, as suggested in reaction 2.

$$[VO(L)_4]^{2+} + H_2O \rightarrow [VO(L)_3(H_2O)]^{2+} + L \qquad (2)$$

The relative intensity of the $[VOOH(L)_2]^+$ species decreased from 100% for acn to ca. 60%, 20%, and 5% for pn, bn, and bzn, respectively, and similar decreases in relative intensity were observed for the protonated nitrile products (*m*/*z* 56, 70, and 104 for pn, bn, and bzn, respectively). For the larger nitriles, the preferred dissociation pathway became the one in which $[VO(L)_3]^{2+}$ and the H_2O adduct were formed. The tendency of $[VO(L)_3]^{2+}$ to generate the H_2O adduct was significantly higher for the larger nitriles compared to acn. With respect to the nitrile ligand, the tendency for direct H_2O addition to $[VO(acn)_3]^{2+}$ followed the trend bn > bzn > pn. The tendency for enhanced H_2O addition for complexes with comparatively larger ligands is consistent with earlier studies by our group of the hydration of Ag^+ [52] and UO_2^{2+} [46,47] complexes. We attribute the higher intrinsic hydration tendencies for complexes with larger ligands to the increased number of vibrational degrees of freedom with the larger ligand. A larger number of oscillators can better accommodate the exothermicity of the association reaction by decreasing the rates of the reverse (dissociation) reactions and thus enabling adduct stabilization. The trend with respect to the nitrile ligands observed when comparing the additions of a single H_2O ligand to $[VO(L)_3]^{2+}$ suggests that the increase in the number of degrees of freedom in the pn or bn complexes enhances hydration compared to acn complexes, but that increasing basicity and/or steric hindrance might be responsible for decreasing H_2O addition to bzn complexes when compared to bn complexes. On the other hand, the enhanced propensity of bn to add H_2O would also be consistent with a larger number of low-lying torsional modes in bn compared to bzn. A similar influence of the nitrile on the formation of H_2O adducts was observed in our earlier investigation of uranyl−nitrile complex ions.[50]

Subsequent CID of $[VO(L)_3]^{2+}$ and $[VO(L)_3(H_2O)]^{2+}$ (MS^3 stage, spectra not shown) led primarily to $[VOOH(L)_2]^+$ product ions. For the $[VO(L)_3]^{2+}$ precursor ion, the formation of the hydroxide product ion presumably occurs through a process similar to that proposed in reaction 1, without the elimination of the neutral nitrile ligand. It is interesting to note that some $[VOOH(L)_2]^+$ was generated from $[VO(L)_3]^{2+}$ (along with $[VO(L)_3(H_2O)]^{2+}$ and $[VO(L_3)(H_2O)_2]^{2+}$) even when the latter species was isolated and stored in the ion trap (spectra not shown), but not collisionally activated, for 30 ms. This observation suggests that the activation barrier for the reaction to produce $[VOOH(L)_2]^+$ from $[VO(L)_3]^{2+}$ is very low. Formation of $[VOOH(L)_2]^+$ by the CID of $[VO(L)_3(H_2O)]^{2+}$ might involve dissociation of the H_2O ligand, proton transfer to a nitrile ligand, elimination of the protonated nitrile, and retention of the OH^- by the vanadyl ion, as suggested in reaction 3.

$$[VO(L)_3(H_2O)]^{2+} \rightarrow [VOOH(L)_2(L + H)]^{2+*} \rightarrow [VOOH(L)_2]^+ + (L + H)^+ \qquad (3)$$

Unlike the result for $[VO(L)_3]^{2+}$, isolation and storage of $[VO(L)_3(H_2O)]^{2+}$ without imposed collisional activation led to the addition of a single H_2O ligand rather than the generation of the ligated $[VOOH(L)_2]^+$ products.

CID of $[VOOH(L)_2]^+$. Figure 3 shows the product-ion mass spectra generated by the CID of $[VOOH(L)_2]^+$(MS/MS stage). The product-ion spectra were generated by isolating the precursor ion for CID directly from the ESI spectrum. Similar product-ion spectra, with respect to the *m*/*z* ratios of the ions and their relative intensities, were observed when $[VOOH(L)_2]^+$ was first generated from $[VO(L)_4]^{2+}$ (MS/MS stage) and then subjected to a subsequent dissociation step (MS^3 stage). CID of $[VOOH(L)_2]^+$ led to three general product ions: (1) $[VOOH(L)]^+$ via elimination of a single nitrile ligand (product ions at *m*/*z* 125, 139, 153, and 187 for L = acn, pn, bn, and bzn, respectively), (2) $[VOOH(L)(H_2O)]^+$ via addition of H_2O in the gas phase, and (3) a product ion 32 u higher in mass than the $[VOOH(L)]^+$ species. The fact that both the hydrated product, $[VOOH(L)(H_2O)]^+$, and the species 32 u higher in mass were adducts to $[VOOH(L)]^+$ was confirmed by isolating $[VOOH(L)]^+$, without imposed collision activation, in the ion trap after it had been generated from $[VOOH(L)_2]^+$ by CID (spectra not shown).

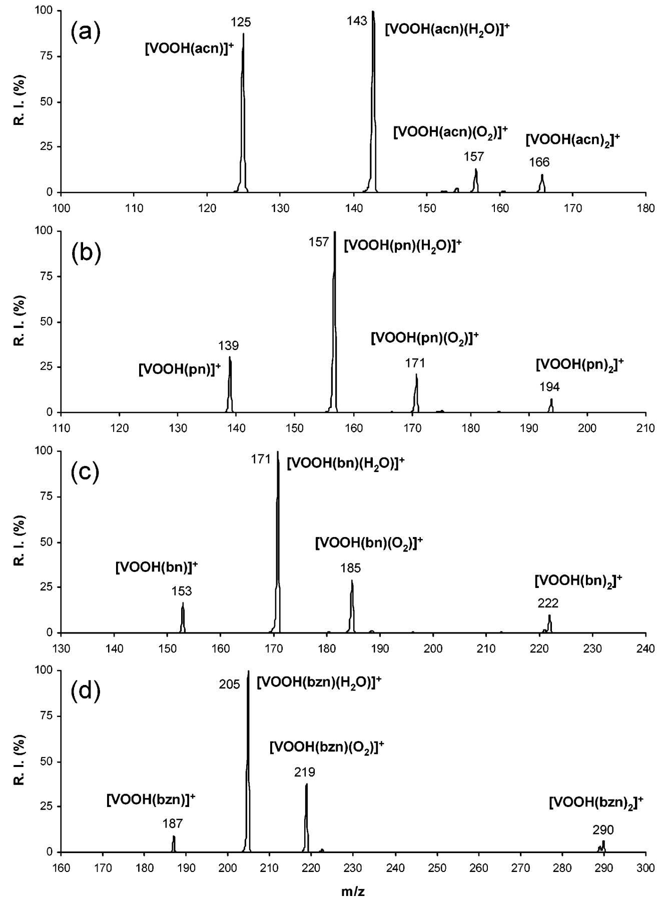

Figure 3. Collision-induced dissociation spectra of $[VOOH(L)_2]^{2+}$, where L corresponds to (a) acetonitrile, (b) propionitrile, (c) butyronitrile, and (d) benzonitrile.

The addition of 32 u in mass could represent the formation of either a CH_3OH or an O_2 adduct to $[VOOH(L)]^+$. The resolving power and mass measurement accuracy of the ion trap are not sufficient to distinguish between the two products. In addition, the peak corresponding to the addition of 32 u to $[VOOH(L)]^+$ displayed an increased width and chemical mass shift characteristic of loosely bound adducts in the ion-trap experiment: these factors prohibited an identification of the adduct identity by *m*/*z* measurement alone. CH_3OH could arise because of trace amounts of solvent remaining in the solution-transfer capillaries and in the vacuum system from experiments conducted prior to those presented here. O_2 is present in the ion trap because ESI is an atmospheric-pressure ionization method and ambient air is sampled into the ion-transmission optics and the vacuum system. The experiments involving CID of $[VOOH(L)_2]^+$ were conducted three separate times, the second two after thorough cleaning of the solution-transfer

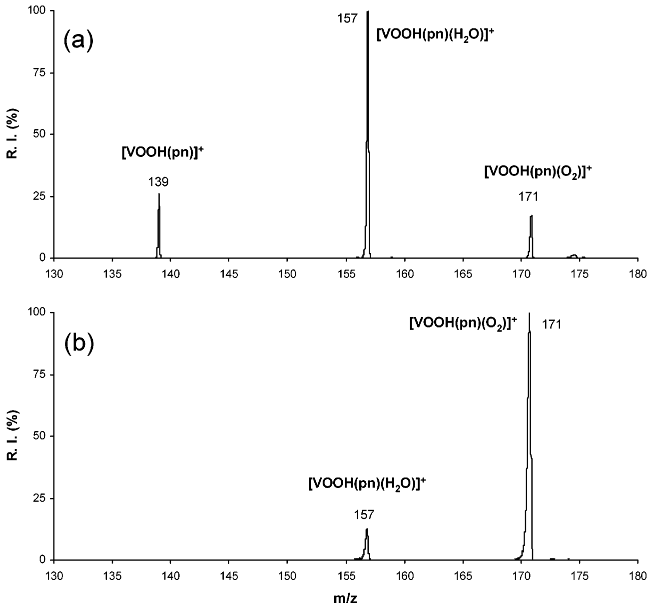

Figure 4. Product-ion mass spectra generated by from $[VOOH(pn)]^+$, initially derived from the CID of $[VOOH(pn)_2]^+$, that was isolated and stored in the ion trap for a period of 100 ms. In a, the species was isolated and stored in a gas-phase environment of He and adventitious O_2. In b, the species was isolated and stored in a gas-phase environment of He with 0.1% molecular O_2.

capillaries and ion optics of the ESI mass spectrometer, thus minimizing the amount of potential CH_3OH contamination. In all three trials, the adduct 32 u higher in mass than $[VOOH(L)]^+$ was observed at relative intensities comparable to those apparent in Figure 3. Figure 4 shows the results of a separate trial in which $[VOOH(pn)]^+$ (*m*/*z* 139) initially derived from CID of $[VOOH(pn)_2]^+$ was isolated and stored in the ion trap for a period of 100 ms. In Figure 4a, $[VOOH(pn)]^+$ was isolated and stored in a gas-phase environment composed of He with adventitious H_2O and O_2 (i.e., an environment similar to the one used to generate the spectra in Figure 3). The partial pressure of O_2 present in the ion trap when the spectrum in Figure 4a was collected is not known, but was determined by the amount of ambient air admitted into the ion trap through the ESI source. To generate the spectrum in Figure 4b, $[VOOH(pn)]^+$ was isolated and stored using a bath gas that was, instead, a certified blend of He with 0.1% molecular O_2. As is apparent in Figure 4b, the product ion at *m*/*z* 171 is significantly higher than both $[VOOH(pn)(H_2O)]^+$ at *m*/*z* 157 and the peak at *m*/*z* 171 Figure 4a. The increase in the peak at *m*/*z* 171 when the He/O_2 gas blend was used identifies the product as a molecular O_2 adduct. The addition of molecular O_2 to the $[VOOH(L)]^+$ species when stored in the ion trap in these experiments is reminiscent of similar chemistry recently reported by our groups for ligated UO_2^+.[10]

CID of $[VOOH(pn)(O_2)]^+$, once formed by an association reaction, caused the elimination of O_2 to form $[VOOH(pn)]^+$ and the hydrated form of the ion, $[VOOH(pn)(H_2O)]^+$. Isolation and storage of $[VOOH(L)(H_2O)]^+$ established that a second H_2O ligand could be added to $[VOOH(L)]^+$. However, addition of O_2 to $[VOOH(L)(H_2O)]^+$ was not observed, even when the He/O_2 blend bath gas was used, nor was the exchange of H_2O for O_2 observed. Isolation and storage of $[VOOH(L)(O_2)]^+$ produced no further adduct species, nor was the exchange of O_2 for H_2O observed. These observations suggest that there exist two coordination sites on the VOOH(L) species for binding additional ligands. Upon isolation and storage of $[VOOH(L)]^+$, those two sites can accommodate up to two monodentate H_2O ligands or a single O_2 molecule presumably bound in a bidentate fashion. Extending the ion isolation and storage times to 1−5 s failed to generate a product ion in which either three H_2O ligands or a combination of a single H_2O and an O_2 ligand were added to $[VOOH(L)]^+$.

Upon dissociation of $[VOOH(L)_2]^+$, the intensity of $[VOOH(L)(H_2O)]^+$ systematically increased with the size of the nitrile ligand, and it was observed at the highest relative intensities for bn and bzn. This observation can be rationalized, in part, using the proposal that accommodation of reaction exothermicity by internal modes in the species with larger, more complex ligands enhances the potential for direct ligand addition (in this case, H_2O addition). However, the tendency to add O_2 rather than H_2O to $[VOOH(L)]^+$ also appears to be dependent on the nitrile ligand, L. For example, the ratio of the ion abundance for the O_2 and H_2O adducts, $[VOOH(L)(O_2)]^+/[VOOH(L)(H_2O)]^+$, was calculated by integrating the respective product-ion peak areas and was found to increase from 0.113 for acn to 0.214, 0.293, and 0.370 for pn, bn, and bzn, respectively. The change in ratio of O_2 versus H_2O addition suggests that the addition of the O_2 molecule is more dependent on the presence of a highly basic ligand in the complex.

Addition of O_2 requires a highly undercoordinated V complex; otherwise, more highly ligated systems (beyond the triligated $[VOOH(L)]^+$) would react in a similar fashion. More highly coordinated systems do not react, which suggests that additional donor ligands interact with orbitals that otherwise would participate in O_2 addition. The selectivity of the O_2 addition can be qualitatively rationalized using the energy-level scheme first proposed for the molecular orbitals of the $[VO(H_2O)_4]^{2+}$ complex in 1962 by Ballhausen and Gray.[57,58] There are a total of four molecular orbitals that function as σ acceptors: the two lowest are of 3d parentage, and the next two are primarily of 4p parentage. The extra electron of the V(IV) complex occupies a molecular orbital of almost pure $3d_{xy}$ character. However, in the case of triligated complexes such as the $[VOOH(L)]^+$ ions, only the two lowest σ-accepting orbitals are occupied. Left unoccupied are the two degenerate orbitals of 4p parentage, which, in the $[VOOH(L)]^+$ ions, would then accommodate the lone unbound valence electron at the V metal center. This orbital would be expected to overlap effectively with the π^* orbital of dioxygen, enabling electron transfer from the metal center to dioxygen, producing a stable V(V) superoxide complex. What is not addressed by this explanation is the apparent bidentate nature of the bound O_2 ligand. The observation that more highly electron-donating nitrile ligands facilitate O_2 addition clearly indicates that additional electron density fosters stronger O_2 binding.

Generation and CID of $[VO_2(L)_2]^+$. As noted in the Experimental Methods section, a solution for ESI that was composed, in part, of dissolved $VO(NO_3)_2$ was created by first combining portions of stock $VOSO_4$ and $Ba(NO_3)_2$ solutions and removing the $BaSO_4$ precipitate. Figure 5a shows a high-resolution (ZoomScan) spectrum highlighting the *m*/*z* region containing $[VOOH(acn)_2]^+$ at *m*/*z* 166 and $[VONO_3(acn)_2]^+$ at *m*/*z* 211. The spectrum was obtained using a spray solution in which 7.5 mL of acn was added to the $VO(NO_3)_2$-containing solution to replicate the 100:1 (nitrile-to-VO^{2+}) solutions used to generate the spectra shown in Figures 1−3. The hypothesis tested was that CID of $[VONO_3(L)_2]^+$ would cause the elimination of NO_2 and the oxidation of VO^{2+} to VO_2^+, thus producing a group of complexes that allow for a comparison of the dissociation behavior of $VOOH^+$ and VO_2^+ ions with the same number and type of nitrile ligands. The normal (lower-resolving-

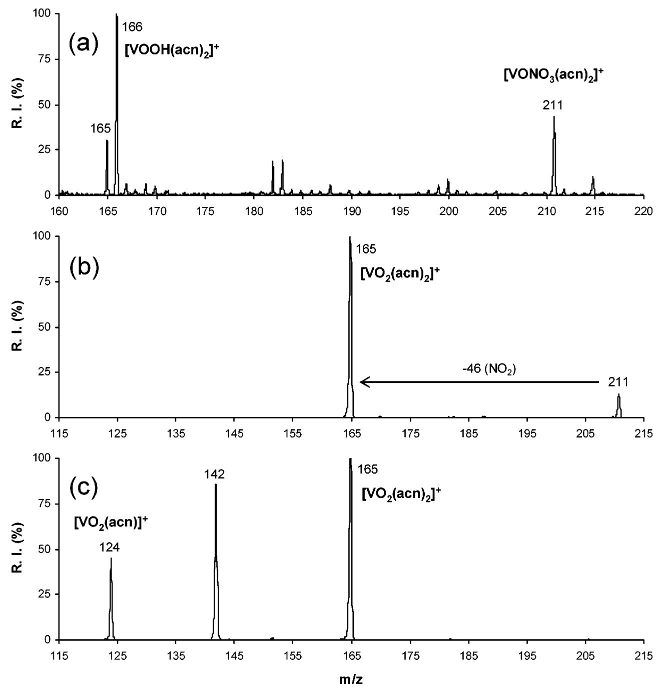

Figure 5. (a) High-resolution scan through the *m*/*z* range highlighting $[VO_2(acn)_2]^+$, $[VOOH(acn)_2]^+$, and $VONO_3(L)_2]^+$. The spectrum was generated using an ESI solution created by mixing $Ba(NO_3)_2$ and $VOSO_4$. (b) CID (MS/MS) of $[VONO_3(L)_2]^+$. (c) CID (MS^3) of $[VO_2(acn)_2]^+$ initially generated by loss of NO_2 from $[VONO_3(L)_2]^+$.

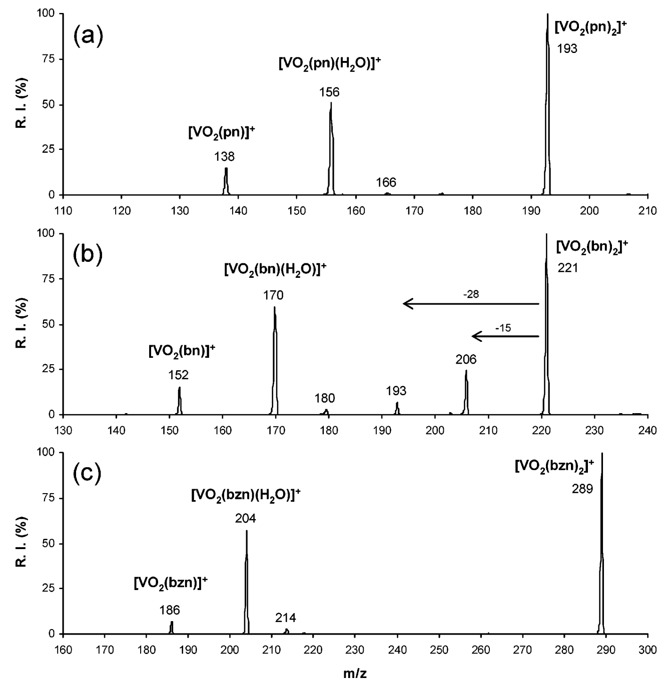

Figure 6. CID (MS^3) of $[VO_2(L)_2]^+$, where L corresponds to (a) propionitrile, (b) butyronitrile, and (c) benzonitrile. In each case, $[VO_2(L)_2]^+$ was generated by loss of NO_2 from $[VONO_3(L)_2]^+$.

power) scan CID spectrum in Figure 5b shows that the CID of $[VONO_3(acn)_2]^+$ (MS/MS stage) at *m*/*z* 211 caused the elimination of 46 u to furnish a single product ion at *m*/*z* 165. The product-ion and neutral-loss masses observed are consistent with the formation of $[VO_2(acn)_2]^+$ via the elimination of NO_2. Subsequent CID of $[VO_2(acn)_2]^+$ (MS^3 stage, Figure 5c) caused the elimination an acn ligand (41 u) to produce $[VO_2(acn)]^+$ at *m*/*z* 124 and a hydrated version of the ion at *m*/*z* 142. CID (MS^4 stage, spectrum not shown) of $[VO_2(acn)]^+$ caused the elimination of the second acn ligand to furnish a peak at *m*/*z* 83, an ion mass consistent with a composition assignment of VO_2^+. The multiple-stage CID results therefore support the composition assignments and production of ligated VO_2^+ from $VONO_3$. The intrinsic chemistry of VO_2^+ was investigated by Schwarz and co-workers, who showed that it did not abstract radicals from either H_2O or organics, a result that is consistent with a singlet electronic structure. The VO_2^+ cation was shown to oxidize olefins to produce aldehydes.[59]

As shown in Figure 5c, CID of $[VO_2(acn)_2]^+$ at *m*/*z* 165 led to the formation of $[VO_2(acn)]^+$ and $[VO_2(acn)(H_2O)]^+$ and *m*/*z* 124 and 142, respectively. Similar CID behavior was observed for the complexes containing pn (Figure 6a), bn (Figure 6b), and bzn (Figure 6c). One notable difference between the CID spectra generated from $[VO_2(L)_2]^+$ and those generated from the VOOH analogues (Figure 3a−d), is the absence in the former of an adduct resulting from the addition of O_2. Instead, a minor peak (<5% relative intensity) was observed 28 u higher in mass than the $[VO_2(L)]^+$ product. We attribute this species to the formation of a N_2 adduct. At no point during the use of our instrument has CO been used as a reagent gas, and we have no good reason to suspect the presence of CO in our instrumental setup. As with O_2, however, some N_2 is expected to be present in the ion trap because ESI is an atmospheric-pressure ionization method and some ambient air is sampled into the vacuum chamber containing the ion-trap mass spectrometer. Identification of the species as an adduct formed by an ion−molecule association reaction was confirmed by monitoring the appearance of the peak 28 u higher in mass after the $[VO_2(L)]^+$ species had been isolated and stored, without imposed collisional activation, after being generated by CID of $[VO_2(L)_2]^+$ (spectra not shown). However, the relative intensity of the N_2 adduct decreased with increased isolation and storage time, and only a weak dependence of the intensity of the N_2 adduct on the identity of the nitrile ligand was observed. The low overall intensity of the adduct suggests that the N_2 ligand is weakly bound to $[VO_2(L)_2]^+$ and is easily removed through collisions with the background gas in the ion trap. For this reason, further attempts to characterize the formation of the molecular N_2 adduct using a He/N_2 blend collision gas were not made.

Although the principal dissociation pathways observed for $[VO_2(L)_2]^+$ was the elimination of intact nitrile ligands, the CID of $[VO_2(bn)_2]^+$ (*m*/*z* 221), as shown in Figure 6c, led to two additional product ions. The first product ion, at *m*/*z* 206, arose via the elimination of 15 u. The second, at *m*/*z* 193, involved the elimination of 28 u. The reaction pathways most likely involve the loss of $-CH_3$ and $CH_2{=}CH_2$, respectively, from one of the bn ligands. The fragmentation mechanisms of amines and nitriles tethered to metal centers are known to be complex.[60] The methyl loss would probably require metal insertion into the $\gamma-\delta$ C−C bond of bn, which would be reminiscent of specific reactions noted for the insertion of Fe^+ into the backbone of longer-chain alkylamine ligands.[61] Such an interpretation draws support from the fact that VO_2^+ complexes containing the other three nitriles (most notably pn) do not participate in these fragmentation reactions.[62]

The last noteworthy observation made during the CID of the $[VO_2(L)_2]^+$ species is that the spectra shown in Figures 5c and 6a−c were generated using the same normalized collision energies (25%) employed for the CID of the $[VOOH(L)_2]^+$ complexes and for the spectra displayed in Figure 3. For the $[VOOH(acn)_2]^+$ and $[VO_2(acn)_2]^+$ complexes, the voltages applied to the end-cap electrodes using a 25% normalized collision energy setting were 0.603 and 0.604 V, respectively. For the $[VOOH(bn)_2]^+$ and $[VO_2(bn)_2]^+$ complexes, the applied voltages were 0.657 and 0.658, respectively. At comparable collision energies, it is clear from a comparison of the spectra in Figures 3 and 6 that dissociation is more facile for the VOOH complexes than for the VO_2 analogues. The basis for this conclusion is the fact that the dominant peaks in the CID spectra obtained from the $[VO_2(L)_2]^+$ complexes, at the collision energies employed, are undissociated precursor ions rather than product ions. For the $[VOOH(L)_2]^+$ species, use of the same normalized collision energies reduced the precursor ion intensities to ca. 10% and resulted in the domination of the CID spectra by the $[VOOH(L)]^+$ and $[VOOH(L)(H_2O)]^+$ product ions. It is assumed, because of the similarities in the precursor-ion compositions and the neutral species eliminated, that the entropy changes associated with the dissociation reactions are comparable. The significant differences in the CID energies required to activate nitrile elimination might therefore reflect different bond energies between nitrile ligand and VO_2^+ or VOOH. This might be due to a combination of greater ion−dipole interactions between the more highly charged V atom in VO_2^+ [formally V(V)] and the nitrile ligands, resulting in a greater transfer of charge from the nitrile ligands to the VO_2^+ center. In comparison, the V atom in VOOH is formally a V(IV) species, and the extra electron at the metal center no doubt serves to repel donor ligands.

Regardless of the nitrile used, $[VO(L)_2]^{2+}$ was not produced in sufficiently high abundance to permit a study of O_2 addition to this species. This prohibits a comparison of the oxygen addition tendencies of $[VO(L)_2]^{2+}$ and $[VOOH(L)]^+$, which are species that presumably have the same core electronic structures and the same numbers of open coordination sites. As noted in an earlier section, the dominant pathway observed for the CID of $[VO(L)_3]^{2+}$ or $[VO(L_3)H_2O]^{2+}$ led to ligated $VOOH^+$ rather than a more simple ligand elimination reaction to generate $[VO(L)_2]^{2+}$.

Conclusions

We have demonstrated that ESI of aqueous solutions containing $VOSO_4$ and a 100-fold molar excess of organonitrile generates gas-phase complex ions containing complexes composed of nitrile-ligated vanadyl (VO^{2+}), vanadyl hydroxide ($VOOH^+$), and vanadium(V) dioxo cations. The dominant species generated by ESI are doubly charged complex ions with the formula $[VO(L)_n]^{2+}$, where L represents the respective nitrile ligands and $n = 4$ and 5. CID of $[VO(L)_5]^{2+}$ caused the elimination of a single nitrile ligand to produce $[VO(L)_4]^{2+}$. For the CID of $[VO(L)_4]^{2+}$, two distinct dissociation pathways were observed. The first involved the elimination of a second nitrile ligand to generate $[VO(L)_3]^{2+}$ and hydrated versions of this complex. The second led to formation of $[VOOH(L)_2]^+$. The second dissociation pathway involved the elimination of one neutral nitrile ligand and a protonated nitrile species; the latter appeared in the product-ion spectrum. Formation of the VOOH species implicates reactive collisions with gas-phase H_2O. CID of $[VONO_3(L)_2]^+$, generated from spray solutions created by mixing $VOSO_4$ and $Ba(NO_3)_2$ (and removing the $BaSO_4$ precipitate), generated $[VO_2(L)_2]^+$ via the elimination of NO_2.

Complexes with the general composition $[VOOH(L)_2]^+$ and $[VO_2(L)_2]^+$ were subjected to CID and ligand-addition studies. Undercoordinated organonitrile complexes of the hydroxy vanadyl cation, $VOOH^+$, a V(IV) complex having a doublet electronic structure, efficiently add dioxygen. This behavior contrasts with that observed for more highly coordinated V(IV) complexes having both 1+ and 2+ charge states and for organonitrile complexes of the VO_2^+ cation [a V(V) species]. As in previous research on ligated $[UO_2]^+$ (a monocation similarly having a doublet electron configuration), the presence or absence of donor ligands significantly influences the propensity of the doublet metal center to add dioxygen. The presence of more electron-donating donor ligands significantly increases the reactivity of the metal center; however, if too many donor ligands are present, then the addition of dioxygen is halted. The results suggest that only very specifically configured vanadyl metal centers are reactive.

In considering the extent of ligation, it is surprising that the dioxygen adduct did not add an additional water ligand: isolation of $[VOOH(L)]^+$ led to the addition of either a single dioxygen or two H_2O molecules. A self-consistent explanation is that (a) dioxygen adds and interacts as a bidentate ligand and hence (b) occupies two coordination sites of the VOOH cation. These explanations should motivate a detailed computational modeling study.

Acknowledgment. This work was supported, in part, with funds from the National Science Foundation (Grant CHE-0239800) and Wichita State University. G.S.G. and G.L.G. acknowledge support from the U.S. Department of Energy, Environmental Systems Research Program, under Contract DE-AC-07-99ID13727. Funds for the purchase of the LCQ-Deca instrument were provided by the Kansas NSF EPSCoR program and the Wichita State University College of Liberal Arts and Sciences.

References and Notes

(1) Vaska, L. *Acc. Chem. Res.* **1976**, *9*, 175.
(2) Basolo, F.; Hoffman, B. M.; Ibers, J. A. *Acc. Chem. Res.* **1975**, *8*, 384.
(3) Jones, R. D.; Summerville, D. A.; Basolo, F. *Chem. Rev.* **1979**, *79*, 139.
(4) Valentine, J. S. *Chem. Rev.* **1973**, *73*, 235.
(5) Momenteau, M.; Reed, C. A. *Chem. Rev.* **1994**, *94*, 659.
(6) Jacobson, D. B.; Freiser, B. S. *J. Am. Chem. Soc.* **1986**, *108*, 27.
(7) Fiedler, A.; Kretzschmar, I.; Schroder, D.; Schwarz, H. *J. Am. Chem. Soc.* **1996**, *118*, 9941.
(8) Davis, M. I.; Wasinger, E. C.; Decker, A.; Pau, M. Y. M.; Vallaincourt, F. H.; Bolin, J. T.; Eltis, L. D.; Hedman, B.; Hodgson, K. O.; Solomon, E. I. *J. Am. Chem. Soc.* **2003**, *125*, 11214.
(9) Kim, S. O.; Sastri, C. V.; Seo, M. S.; Kim, J.; Nam, W. *J. Am. Chem. Soc.* **2005**, *127*, 4178.
(10) Groenewold, G. S.; Cossel, K. C.; Gresham, G. L.; Gianotto, A. K.; Appelhans, A. D.; Olson, J. E.; Van Stipdonk, M. J.; Chien, W. *J. Am. Chem. Soc.* **2006**, *107*, 3075.
(11) Crans, D. C.; Smee, J. J.; Gaidamauskas, E.; Yang, L. *Chem. Rev.* **2004**, *104*, 849.
(12) Vilter, H. *Metal Ions Biol. Syst.* **1995**, *31*, 325.
(13) Taylor, S. W.; Kammerer, B.; Bayer, E. *Chem. Rev.* **1997**, *97*, 333.
(14) Van Pee, K.-H.; Keller, S.; Wage, T.; Wynands, I.; Schnerr, H.; Zehner, S. *Biol. Chem.* **2000**, *381*, 1.
(15) Butler, A. *Coord. Chem. Rev.* **1999**, *187*, 17.
(16) Butler, A.; Baldwin, H. In *Structure and Bonding—Metal Sites in Proteins and Models*; Springer-Verlag: Berlin, 1997; Vol. 89, p 109.
(17) Sigel, H.; Sigel, A. *Vanadium and Its Role in Life*; Marcel Dekker: New York, 1995; Vol. 31.
(18) Conte, V.; Bortolini, O.; Carraro, M.; Moro, S. *J. Inorg. Biochem.* **2000**, *80*, 41.
(19) Bortolini, O.; Conte, V. *J. Inorg. Biochem.* **2005**, *99*, 1549.
(20) Maurya, M. R.; Agarwal, S.; Bader, C.; Ebel, M.; Rehder, D. *Dalton Trans.* **2005**, *3*, 527.
(21) Stankiewicz, P. J.; Tracey, A. S. *Metal Ions Biol. Syst.* **1995**, *31*, 249.
(22) Rao, C. N. R.; Raven, B. *Transition Metal Oxides*; VCH: New York, 1995.
(23) *Appl. Catal. A* **1997**, *157* (entire volume devoted to metal oxide catalysts).
(24) Greenwood, N. N.; Earnshaw, A. *Chemistry of the Elements*, 2nd ed.; Butterworth-Heinemann: Oxford, U.K., 1997.
(25) Bell, R. C.; Zemski, K. A.; Castleman, A. W., Jr. *J. Phys. Chem. A* **1999**, *102*, 8293.

(26) Bell, R. C.; Zemski, K. A.; Castleman, A. W., Jr. *J. Phys. Chem. A* **1998**, *103*, 2992.
(27) Zemski, K. A.; Justes, D. R.; Castleman, A. W., Jr. *J. Phys. Chem. A* **2001**, *105*, 10237.
(28) Bell, R. C.; Zemski, K. A.; Justes, D. R.; Castleman, A. W., Jr. *J. Phys. Chem. A* **2001**, *114*, 799.
(29) Justes, D. R.; Mitric, R.; Moore, N. A.; Bonacic-Koutecky, V.; Castleman, A. W., Jr. *J. Am. Chem. Soc.* **2003**, *125*, 6289.
(30) Feyel, S.; Schroder, D.; Schwarz, H. *J. Phys. Chem. A* **2006**, *110*, 2647.
(31) Kaczorowska, M.; Schröder, D.; Schwarz, H. *Eur. J. Inorg. Chem.* **2005**, 2919.
(32) Schröder, D.; Loos, J.; Engeser, M.; Schwarz, H.; Jankowiak, H.-C.; Berger, R.; Thissen, R.; Dutuit, O.; Döbler, J.; Sauer, J. *Inorg. Chem.* **2004**, *43*, 1976.
(33) Engeser, M.; Schlangen, M.; Schröder, D.; Schwarz, H. *Organometallics* **2003**, *22*, 3933.
(34) Engeser, M.; Weiske, T.; Schroder, D.; Schwarz, H. *J. Phys. Chem. A* **2003**, *107*, 2855.
(35) Schröder, D.; Engeser, M.; Schwarz, H.; Harvey, J. N. *ChemPhysChem* **2002**, *3*, 584.
(36) Fielicke, A.; Rademann, K. *Phys. Chem. Chem. Phys.* **2002**, *4*, 2621.
(37) Asmis, K.; Santambrogio, G.; Brümmer, M.; Sauer, J. *Angew. Chem., Int. Ed. Engl.* **2005**, *44*, 3122.
(38) Asmis, K.; Meijer, G.; Brümmer, M.; Kaposta, C.; Santambrogio, G.; Wöste, L.; Sauer, J. *J. Chem. Phys.* **2004**, *120*, 6461.
(39) Fielicke, A.; Mitric, R.; Meijer, G.; Bonacic-Koutecky, V.; von Helden, G. *J. Am. Chem. Soc.* **2003**, *125*, 15716.
(40) Muller, A.; Benninghoven, A. *Surf. Sci.* **1973**, *39*, 427.
(41) Rodgers, M. T.; Armentrout, P. B. *Mass Spectrom. Rev.* **2000**, *19*, 215.
(42) Armentrout, P. B. *Annu. Rev. Phys. Chem.* **2001**, *52*, 423.
(43) Dinca, A.; Davis, T. P.; Fisher, K. J.; Smith, D. R.; Willett, G. D. *Int. J. Mass Spectrom. Ion Process.* **1999**, *183*, 73.
(44) Schröder, D.; Engeser, M.; Bronstrup, M.; Daniel, C.; Spandl, J.; Hartl, H. *Int. J. Mass Spectrom.* **2003**, *228*, 743.
(45) Bortolini, O.; Conte, V.; Di Furia, F.; Moro, S. *Eur. J. Inorg. Chem.* **1998**, 1193.
(46) Van Stipdonk, M.; Anbalagan, V.; Chien, W.; Gresham, G.; Groenewold, G.; Hanna, D. *J. Am. Soc. Mass Spectrom.* **2003**, *14*, 1205.
(47) Chien, W.; Anbalagan, V.; Zandler, M.; Hanna, D.; Van Stipdonk, M.; Gresham, G.; Groenewold, G. *J. Am. Soc. Mass Spectrom.* **2004**, *15*, 777.
(48) Groenewold, G. S.; Van Stipdonk, M. J.; Gresham, G. L.; Chien, W.; Bulleigh, K.; Howard, A. *J. Mass Spectrom.* **2004**, *39*, 752.
(49) Van Stipdonk, M. J.; Chien, W.; Angalaban, V.; Bulleigh, K.; Hanna, D.; Groenewold, G. S. *J. Phys. Chem. A* **2004**, *108*, 10448.
(50) Van Stipdonk, M. J.; Chien, W.; Bulleigh, K.; Wu, Q.; S., G. G. *J. Phys. Chem. A* **2006**, *110*, 959.
(51) Lias, S. G.; Bartmess, J. E.; Liebman, J. F.; Holmes, J. L.; Levin, R. D.; Mallard, W. G. *NIST Chemistry WebBook, NIST Standard Reference Database Number 69*; National Institute of Standards and Technology (NIST): Gaithersburg, MD, 2005.
(52) Hanna, D.; Silva, M.; Morrison, J.; Tekarli, S.; Anbalagan, V.; Van Stipdonk, M. J. *J. Phys. Chem. A* **2003**, *107*, 5528.
(53) Vachet, R. W.; Hartman, J. A. R.; Callahan, J. H. *J. Mass Spectrom.* **1998**, *33*, 1209.
(54) Vachet, R. W.; Callahan, J. H. *J. Mass Spectrom.* **2000**, *35*, 311.
(55) Vachet, R. W.; Hartman, J. R.; Gertner, J. W.; Callahan, J. H. *Int. J. Mass Spectrom.* **2001**, *204*, 101.
(56) Combariza, M. Y.; Vachet, R. W. *J. Am. Soc. Mass Spectrom.* **2002**, *13*, 813.
(57) Ballhausen, C. J.; Gray, H. B. *Inorg. Chem.* **1962**, *1*, 111.
(58) Bernal, I.; Rieger, P. H. *Inorg. Chem.* **1963**, *3*, 256.
(59) Harvey, J. N.; Diefenbach, M.; Schroder, D.; Schwarz, H. *Int. J. Mass Spectrom. Ion Process.* **1999**, *183*, 85.
(60) Schwarz, H. *Acc. Chem. Res.* **1989**, *22*, 282.
(61) Karrass, S.; Schwarz, H. *Helv. Chim. Acta* **1989**, *72*, 633.
(62) Schroder, D.; Schwarz, H. *Angew. Chem., Int. Ed. Engl.* **1995**, *34*, 1973.